Journal of Organometallic Chemistry 694 (2009) 3643–3652

Contents lists available at ScienceDirect

Journal of Organometallic Chemistry

journal homepage: www.elsevier.com/locate/jorganchem

Structures, preparation and catalytic activity of ruthenium cyclopentadienyl complexes based on pyridyl-phosphine ligand

Prashant Kumar, Ashish Kumar Singh, Sanjeev Sharma, Daya Shankar Pandey *

Department of Chemistry, Faculty of Science, Banaras Hindu University, Varanasi 221 005, UP, India

ARTICLE INFO

Article history:
Received 10 April 2009
Received in revised form 1 July 2009
Accepted 6 July 2009
Available online 14 August 2009

Keywords:
Ruthenium complexes
Cyclopentadienyl
Diphenyl-2-pyridylphosphine (PPh_2Py)
Dimethylglyoxime
1,2-Phenylenediamine

ABSTRACT

Ruthenium complexes $[(\eta^5\text{-}C_5H_5)Ru(\kappa^1\text{-}P\text{-}PPh_2Py)(PPh_3)Cl]$ (**1**) and $[(\eta^5\text{-}C_5H_5)Ru(\kappa^2\text{-}P,N\text{-}PPh_2Py)(PPh_3)]^+$ (**1a**) containing diphenyl-2-pyridylphosphine (PPh_2Py) are reported. Coordinated PPh_2Py in the complex $[(\eta^5\text{-}C_5H_5)Ru(\kappa^1\text{-}P\text{-}PPh_2Py)(PPh_3)Cl]$ (**1**) exhibits monodentate behavior. In presence of NH_4PF_6 in methanol at room temperature it afforded chelated complex $[(\eta^5\text{-}C_5H_5)Ru(\kappa^2\text{-}P,N\text{-}PPh_2Py)(PPh_3)]^+$ (**1a**). Further, **1** reacted with various species viz., CH_3CN, NaCN, NH_4SCN and NaN_3 to afford cationic and neutral complexes $[(\eta^5\text{-}C_5H_5)Ru(\kappa^1\text{-}P\text{-}PPh_2Py)(PPh_3)L]^+$ and $[(\eta^5\text{-}C_5H_5)Ru(\kappa^1\text{-}P\text{-}PPh_2Py)(PPh_3)L]$ [L = CH_3CN (**1b**); CN^- (**1c**); N_3^- (**1d**) and SCN^- (**1e**)] and it's reaction with *N,N*-donor chelating ligands dimethylglyoxime (H_2dmg) and 1,2-phenylenediamine (pda) gave cationic complexes $[(\eta^5\text{-}C_5H_5)Ru(\kappa^1\text{-}P\text{-}PPh_2Py)(\kappa^2\text{-}N\text{-}N)]PF_6$ [κ^2-*N*-*N* = dmg (**1f**) and pda (**1g**)]. The complexes **1–1g** have been characterized by physicochemical techniques and crystal structures of **1**, **1a, 1c**, **1e** and **1f** have been determined by single crystal X-ray analyses. Catalytic potential of the complex **1** has been evaluated in water under aerobic conditions. It was observed that the complex **1** selectively catalyzes reduction of aldehyde into alcohol.

1. Introduction

Cyclopentadienyl group has proved to be one of the most ubiquitous and important ligands in organometallic chemistry [1,2]. Ruthenium complexes containing cyclopentadienyl group have been the subject of investigation by many research groups during past couple of decades because of their potential use as starting materials and widespread applications in transition metal-catalyzed asymmetric syntheses [3–11]. Catalytic activity of the ruthenium cyclopentadienyl complexes ranges from hydrogen transfer to ring closing metathesis [12–14]. Further, anti-tumor activity exhibited by some water-soluble arene ruthenium(II) complexes have also evoked immense current interest [15–18].

To control the structure and reactivity, attempts have been made to synthesize ruthenium cyclopentadienyl complexes with additional intra-molecularly tethered coordinating groups [19–23]. Synthetic approaches to such complexes typically falls into one of the two broad categories: (i) synthesis of functionalized cyclopentadienes followed by coordination to the metal, or (ii) anchoring of an additional donor ligand to an already formed cyclopentadienyl complex [19–24]. We feel that the latter approach is more versatile albeit less explored [25–29].

Further, to widen range of available potential platinum group metal complex catalysts it may be interesting to examine possibility of the substitution of ligands bonded to ruthenium center in η^5-cyclopentadienyl ruthenium complexes by a monodentate/chelating phosphine like PPh_2Py [19,30]. In this direction attempts were made to synthesize ruthenium cyclopentadienyl complexes containing PPh_2Py. Phosphines are among the most important ligands in organometallic chemistry with a wide range of steric and electronic properties. In this work attention has been focused mainly on diphenyl-2-pyridylphosphine, a versatile ligand which may coordinate to metal center in monodentate, chelating or bridging manner, depending upon requirements at the reaction center [31–35]. We describe herein reproducible syntheses, characterization and reactivity of ruthenium cyclopentadienyl complexes based on diphenyl-2-pyridylphosphine (PPh_2Py). Also, we present herein molecular structures of the complexes **1**, **1a, 1c**, **1e** and **1f** and results of our studies on catalytic activity of **1** in the reduction of aldehyde to alcohol under aqueous and aerobic conditions [36,37].

2. Experimental

2.1. Materials and physical measurements

Analytical grade chemicals were used throughout. Solvents were dried and distilled before use following standard literature

* Corresponding author. Tel.: + 91 542 6702480.
E-mail address: dspbhu@bhu.ac.in (D.S. Pandey).

0022-328X/$ - see front matter © 2009 Elsevier B.V. All rights reserved.
doi:10.1016/j.jorganchem.2009.07.011

procedures [38]. Hydrated ruthenium (III) chloride, dicyclopentadiene, triphenylphosphine, ammonium tetrafluoroborate and diphenyl-2-pyridylphosphine were obtained from Aldrich Chemical Company, Inc. USA and were used without further purifications. The precursor complex $[(\eta^5\text{-}C_5H_5)Ru(PPh_3)_2Cl]$ was prepared and purified by the literature procedure [39].

Elemental analyses on the complexes were performed by micro analytical laboratory of the Sophisticated Analytical Instrument Facility, Central Drug Research Institute, Lucknow. Infrared spectra in KBr discs in the region 4000–400 cm^{-1} and electronic spectra were recorded on a Shimadzu-8201 PC and Shimadzu UV-1601 spectrophotometers, respectively. ^1H NMR spectra with tetramethylsilane as the internal reference and $^{31}P\{^1H\}$ NMR with H_3P0_4(85%) as the external reference were obtained at room temperature on a Bruker DRX-300 NMR machine. Electrochemical experiments were carried out in an airtight single compartment cell using platinum as the counter electrode, glassy carbon as the working electrode and Ag/Ag+ reference electrode on a CHI 620c electrochemical analyzer. Fast atom bombardment (FAB) and ESI mass spectra were recorded on a JOEL SX 102/DA-6000 Mass spectrometer using Xenon as the FAB gas (6 kV, 10 mA). The accelerating voltage was 10 kV and spectra were recorded at room temperature using *m*-nitrobenzyl alcohol as the matrix.

2.2. Syntheses

2.2.1. Preparation of $[(\eta^5\text{-}C_5H_5)Ru(\kappa^1\text{-}P\text{-}N\text{-}PPh_2Py)(PPh_3)]$ **1**

A mixture of $[(\eta^5\text{-}C_5H_5)Ru(PPh_3)_2Cl]$ (0.5 g, 0.68 mmol) and PPh_2Py (0.18 g, 0.68 mmol) in benzene (25 ml) was heated under reflux 8 h. After cooling to room temperature, benzene was removed under vacuo and resulting orange residue was subjected to purification by flash silica gel chromatography (CH_2Cl_2/ethylacetate, 3/1 v/v). It afforded compound **1** as an orange solid. The orange solid was recrystallised from CH_2Cl_2-petroleum ether (40–60). Yield: 0.598 g, 69%. M.P. 145 °C Microanalytical data: $C_{40}H_{34}Cl_4NP_2Ru$, requires: C, 57.64; H, 4.11; N, 1.68. Found: C, 57.58; H, 4.24; N, 1.34%. ESI-MS(calcd): *m*/*z* 691.2 (690), $[(\eta^5\text{-}C_5H_5)Ru(\kappa^2\text{-}P\text{-}N\text{-}PPh_2Py)(PPh_3)]^+$; 429.2 (427), $[(\eta^5\text{-}C_5H_5)Ru(\kappa^2\text{-}P\text{-}N\text{-}PPh_2Py)]^+$. ^1H NMR ($CDCl_3$, TMS, δ, ppm): 7.72–6.65 (m, 15H, PPh_3), 4.68 (s, 5H, $\eta^5\text{-}C_5H_5$), 7.24–7.08 (br. m, 14H, aromatic protons of PPh_2Py), 7.90 (t, 1H, J_{H-H} = 4.36 Hz), 8.11 (t, 1H, J_{H-H} = 4.42 Hz), 8.67 (d, 1H, J = 5.12 Hz), $^{31}P\{^1H\}$ NMR ($CDCl_3$, H_3PO_4, δ, ppm): 59.72 (s, PPh_2Py) and 54.90 (s, PPh_3) ppm. IR (cm^{-1}, KBr pellet): 1626 (s), 1440 (s), 1394 (m), 1102 (m), 844 (s), 758 (s), 698(s. UV–Vis, λ_{max}, nm (ε): 240 (37 728), 264 (13 540), 308 (5500), 391(3140).

2.2.2. Synthesis of $[(\eta^5\text{-}C_5H_5)Ru(\kappa^2\text{-}P\text{-}N\text{-}PPh_2Py)(PPh_3)]PF_6$ **1a**

2.2.2.1. Method 1. The complex $[(\eta^5\text{-}C_5H_5)Ru)(PPh_3)_2Cl]$ (0.108 g, 0.149 mmol) in methanol (25 mL) was treated with diphenyl-2-pyridylphosphine (PPh_2Py) (0.196 g, 0.748 mmol) and NH_4PF_6 (0.078 g, 0.748 mmol) and contents of the flask were stirred at room temperature for 2 h. Slowly, it dissolved and gave a yellow solution. It was filtered to remove any solid impurities and concentrated to half its volume and left for slow crystallization in a refrigerator. Slowly, microcrystalline product separated, which was filtered washed with diethyl ether and dried *in vacuo*. Yield: 0.611 g, 72%. M.P. 140 °C, Microanalytical data: $PC_{40}F_6H_{34}N_1P_2Ru$, requires: C, 61.71; H, 4.40; N, 1.80. Found: C, 61.58; H, 4.74; N, 1.34%. ESI-MS(calcd).: *m*/*z* 727 (726), $[Ru(\eta^5\text{-}C_5H_5)(\kappa^1\text{-}P\text{-}N\text{-}PPh_2Py)(PPh_3)Cl]$; 465 (464), $[(\eta^5\text{-}C_5H_5)Ru(\kappa^2\text{-}P\text{-}N\text{-}PPh_2Py)Cl]$. ^1H NMR ($CDCl_3$,TMS δ, ppm): 7.82–6.95 (m, 15H, PPh_3), 4.70 (s, 5H, $\eta^5\text{-}C_5H_5$), 7.26–7.04 (br. m, 14H, aromatic proton of PPh_2Py), 7.89 (t, 1H, J_{H-H} = 4.36 Hz), 8.01 (t, 1H, J_{H-H} = 4.42 Hz), 8.67 (d, 1H, J = 5.12 Hz), $^{31}P\{^1H\}$ NMR ($CDCl_3$, H_3PO_4 δ, ppm): −11.25 (s, PPh_2Py) and 41.54 (s, PPh_3) ppm. IR (cm^{-1}, KBr pellet): 1626 (s), 1440 (s), 1394 (m), 1102 (m), 844 (s), 758 (s), 698(s), $\nu(PF_6^-)$ 840 cm^{-1}. UV–Vis, λ_{max}, nm (ε): 242 (37 730), 268 (13 640), 308 (5500), 391(3140).

2.2.2.2. Method 2. To a suspension of $[(\eta^5\text{-}C_5H_5)Ru(\kappa^1\text{-}P\text{-}PPh_2Py)(PPh_3)Cl]$ (**1**) (0.108 g, 0.149 mmol) in methanol (25 mL) NH_4PF_6 (0.078 g, 0.748 mmol) was added and stirred at room temperature for 8 h. The clear orange yellow solution was then rotatory evaporated. Residue was extracted with dichloromethane and filtered to remove any insoluble material. From the filtrate **1a** was isolated in ~70% yield.

2.2.3. Synthesis of $[(\eta^5\text{-}C_5H_5)Ru(\kappa^1\text{-}P\text{-}PPh_2Py)(PPh_3)(NCCH_3)]BF_4$ **1b**

To a suspension of complex **1** (0.06 g, 0.092 mmol) in acetonitrile (15 ml) NH_4BF_4 (0.019 g, 0.184 mmol) was added and refluxed under a nitrogen atmosphere for 2 h, whereupon the yellow solution turned pale yellow in color. The solvent was rotatory evaporated and yellow mass thus obtained was dissolved in CH_2Cl_2 and filtered. The filtrate was concentrated to 2 ml and hexane was added to induce precipitation. The light yellow product was washed with diethyl ether and dried under vacuum. Yield: 0.724 g, 78%. M.P. 155 °C, Microanalytical data: $BC_{42}F_4H_{38}N_2P_2Ru$, requires: C, 61.47; H, 4.67; N, 3.41%. Found: C, 61.41; H, 4.62; N, 3.39%. 1H NMR ($CDCl_3$, TMS, δ, ppm): 7.82–6.95 (m, 15H, PPh_3), 2.18 (s, 3H, CH_3), 4.70 (s, 5H, $\eta^5\text{-}C_5H_5$), 7.26–7.04 (br. m, 14H, aromatic proton of PPh_2Py), 7.89 (t, 1H, J_{H-H} = 4.36 Hz), 8.01 (t, 1H, J_{H-H} = 4.42 Hz), 8.67 (d, 1H, J = 5.12 Hz), $^{31}P\{^1H\}$ NMR ($CDCl_3$, H_3PO_4 δ, ppm): 59.72 (s, PPh_2Py), 54.90 (s, PPh_3). IR (cm^{-1}, KBr): 2324(s), 1626 (s), 1440 (s), 1394 (m), 1102 (m), 844 (s), 758 (s), 698 (s), $\nu(BF_4^-)$ 1056 cm^{-1}. UV–Vis, λ_{max}, nm (ε): 240 (35 550), 272 (13 080), 398 (2900), 434 (2810).

2.2.4. Synthesis of $[(\eta^5\text{-}C_5H_5)Ru(\kappa^1\text{-}P\text{-}PPh_2Py)(PPh_3)CN]$ **1c**

A mixture of complex **1** (0.06 g, 0.092 mmol) and sodium cyanide (NaCN) (0.048 g, 0.23 mol) in methanol (15 ml) were refluxed for 3 h. The yellow suspension gradually turned light yellow in color. Solvent was removed under reduced pressure and the yellowish solid was dissolved in CH_2Cl_2 and filtered. The filtrate was concentrated to 2 ml and left for slow crystallization in a refrigerator. Slowly, a yellow microcrystalline product separated which was filtered, washed with diethyl ether and dried under vacuum. Yield: 0.624 g, 72%. M.P. 150 °C, Microanalytical data: $C_{41}H_{34}N_2P_2Ru$, requires: C, 61.21; H, 4.26; N, 3.48. Found: C, 61.18; H, 4.24; N, 3.42%. ^1H NMR ($CDCl_3$, δ): ^1H NMR ($CDCl_3$, TMS, δ. ppm): 7.82–6.95 (m, 15H, PPh_3), 4.70 (s, 5H, $\eta^5\text{-}C_5H_5$), 7.26–7.04 (br. m, 14H, aromatic proton of PPh_2Py), 7.89 (t, 1H, J_{H-H} = 4.36 Hz), 8.01 (t, 1H, J_{H-H} = 4.42 Hz), 8.67 (d, 1H, J = 5.12 Hz), $^{31}P\{^1H\}$ NMR ($CDCl_3$, H_3PO_4 δ, ppm): 57.82 (s, PPh_2Py), 54.90 (s, PPh_3). IR (cm^{-1}, nujol): 2227 (s), 1626 (s), 1440 (s), 1394 (m), 1102 (m), 844 (s), 758 (s), 698(s). UV–Vis, λ_{max}, nm (ε): 244 (38 470), 268 (13 640), 308 (5500), 388(3270).

2.2.5. Synthesis of $[(\eta^5\text{-}C_5H_5)Ru(\kappa^1\text{-}P\text{-}PPh_2Py)(PPh_3)N_3]$ **1d**

This complex was prepared following the above procedure except that sodium azide (NaN_3) (0.048 g, 0.23 mmol) was used in place of sodium cyanide (NaCN). It isolated in the form of yellow microcrystalline solid. Yield: 0.686 g, 74%, M.P. 155 °C Microanalytical data: $C_{40}H_{35}N_4P_2Ru$ requires: C, 58.48; H, 4.29; N, 6.82. Found: C, 58.44; H, 4.24; N, 6.80%. ^1H NMR ($CDCl_3$, TMS, δ, ppm): 7.82–6.95 (m, 15H, PPh_3), 2.18 (s, 3H, CH_3), 4.70 (s, 5H, $\eta^5\text{-}C_5H_5$), 7.26–7.04 (br. m, 14H, aromatic protons of PPh_2Py), 7.89 (t, 1H, J_{H-H} = 4.36 Hz), 8.01 (t, 1H, J_{H-H} = 4.42 Hz), 8.67 (d, 1H, J = 5.12 Hz). IR (cm^{-1}, nujol): 2042, 1626 (s), 1440 (s), 1394 (m), 1102 (m), 844 (s), 758 (s), 698(s), UV–Vis, λ_{max}, nm (ε): 240 (25 210), 268 (22 320), 308 (10 500), 434(1650).

*2.2.6. Synthesis of [(η^5-C_5H_5)Ru(κ^1-P-PPh_2Py)(PPh_3)(SCN)] **1e***

This complex was prepared following the above procedure except that ammonium thiocyanate (NH_4SCN) (0.048 g, 0.23 mmol) was used in place of sodium azide (NaN_3). It isolated as an orange microcrystalline solid. Yield: 0.721 g, 77%, M.P. 165 °C. Microanalytical data: $C_{41}H_{35}N_2P_2RuS$ requires: C, 58.79; H, 4.21; N, 3.34. Found: C, 58.74; H, 4.26; N, 3.36**%.** FAB-MS (*m*/*z*,(calc) 749.2 (748), [(η^5-C_5H_5)Ru(κ^1-*P*-PPh_2Py)(PPh_3)SCN]; 687 (686), [(η^5-C_5H_5)Ru(κ^1-*P*-PPh_2Py)(PPh_3)]. ^{1}H NMR ($CDCl_3$, δ, ppm): 8.55 (d, 1H, *J* = 5.1 Hz), 7.91 (d, 1H, *J* = 7.8 Hz), 7.74 (m, 7H), 7.61 (t, 1H, *J* = 7.8 Hz), 7.51 (t, 1H, *J* = 8.1 Hz), 7.26–7.04 (br.m, 15H, aromatic proton of PPh_2Py), 6.87 (t, 1H, *J* = 6.3 Hz), 3.88 (t, 1H, *J* = 10.2 Hz), 3.64 (d, 2H, *J* = 13.2 Hz). IR (cm^{-1}, nujol): 2100 (s), 1626 (s), 1440 (s), 1394 (m), 1102 (m), 844 (s), 758 (s), 698(s). UV–Vis, λ_{max}, nm (ε): 241(35 750), 268 (22 320), 365 (3670), 387(3300).

*2.2.7. Synthesis of [(η^5-C_5H_5)Ru(κ^1-P-PPh_2Py)(H_2dmg)]PF_6 **1f***

A suspension of complex **1** (0.135 g, 0.163 mmol) in methanol (20 ml) was treated with dimethylglyoxime (H_2dmg) (0.035 g, 0.326 mmol) and allowed to stir at room temperature for 10 h. It was filtered to remove any solid impurities. A saturated solution of ammonium hexaflorophosphate (0.026 g, 0.162 mmol) dissolved in 5 ml methanol was added to the filtrate and left for slow crystallization in the refrigerator. Slowly, a microcrystalline product separated which was filtered, washed with diethyl ether and dried *in vacuo*. Yield: 0.611 g, 72%. M.P. 160 °C Microanalytical data: $PC_{26}F_6H_{27}N_3PRuO_2$ requires: C, 49.38; H, 4.30; N, 6.64. Found: C, 49.41; H, 4.28; N, 6.59**%.** FAB-MS (*m*/*z*, (calc) 777 (776), [(η^5-C_5H_5)Ru(κ^1-*P*-PPh_2Py)(H_2dmg)]PF_6; 634 (633), [(η^5-C_5H_5)Ru(κ^1-*P*-PPh_2Py)(H_2dmg)]$^+$, 370 (369), [Ru(η^5-C_5H_5)(H_2dmg)]$^+$. ^{1}H NMR ($CDCl_3$, TMS, δ, ppm): 7.82–6.95 (m, 15H, PPh_3), 1.92 (s, 6H, CH_3), 4.70 (s, 5H, η^5-C_5H_5), 7.26–7.04 (br. m, 14H, aromatic proton of PPh_2Py), 7.89 (t, 1H, J_{H-H} = 4.36 Hz), 8.01 (t, 1H, J_{H-H} = 4.42 Hz), 8.67 (d, 1H, *J* = 5.12 Hz), ^{31}P{^{1}H} NMR ($CDCl_3$, H_3PO_4 δ, ppm): 40.04 (s), −142.02 (sept. PF_6). IR (cm^{-1}, KBr): 3400 (s), 1626 (s), 1440 (s), 1394 (m), 1102 (m), 1030 (m), 844 (s), 758 (s), 698 (s), ν(PF_6^-) 840 cm^{-1}. UV–Vis, λ_{max}, nm (ε): 239 (29 600), 267 (10 480), 359 (3710), 398(2900), 409(1765).

*2.2.8. Synthesis of [(η^5-C_5H_5)Ru(κ^1-P-PPh_2Py)(pda)]BF_4 **1g***

This complex was prepared following the above procedure (**1f**) except that 1,2-phenylenediamine (pda) (0.035 g, 0.326 mmol) was used in place of dimethylglyoxime (H_2dmg). It separated as an orange microcrystalline solid and was washed with diethyl ether and dried under vacuum. Yield: 0.672 g, 73%., M.P. 165 °C, Microanalytical data: $BC_{28}F_4H_{27}N_3Pru$ requires: C, 53.86; H, 4.36; N, 6.73%. Found: C, 53.80; H, 4.34; N, 6.74%. ^{1}H NMR ($CDCl_3$, TMS, δ, ppm): 8.20–6.95 (m, 15H, PPh_3), 5.00 (d, 4H, NH_2, J_{H-H} = 12.23 Hz), 4.70 (s, 5H, η^5-C_5H_5), 7.26–7.04 (br. m, 14H, aromatic protons of PPh_2Py), 7.89 (t, 1H, J_{H-H} = 4.36 Hz), 8.01 (t, 1H, J_{H-H} = 4.42 Hz), 8.67 (d, 1H, *J* = 5.12 Hz), ^{31}P{^{1}H} NMR ($CDCl_3$, H_3PO_4 δ, ppm): 40.04 (s). IR (cm^{-1}, nujol): 1626 (s), 1440 (s), 1394 (m), 1102 (m), 844 (s), 758 (s), 698(s), ν(BF_4^-) 1056 cm^{-1} UV–Vis, λ_{max}, nm (ε): 240 (25 210), 268 (22 320), 388 (3270), 403 (1650).

2.3. X-ray crystallography

Suitable crystals for single X-ray diffraction analyses for complexes **1**, **1a, 1c, 1e** and **1f** were obtained from CH_2Cl_2/petroleum ether (40–60 °C) at room temperature by slow diffusion method. Preliminary data on space group and unit cell dimensions as well as intensity data were collected on an OXFORD DIFFRACTION XCAUBER-S' and BRUKER SMART APEX diffractometer using graphite-monochromatized Mo Kα radiation. The structures were solved by direct methods and refined by using SHELX-97 [40]. The non-hydrogen atoms were refined with anisotropic thermal parameters. All the hydrogen atoms are geometrically fixed and allowed to refine using a riding model. The computer program PLATON was used for analyzing the interaction and stacking distance [41].

3. Results and discussion

The complex [(η^5-C_5H_5)Ru(PPh_3)$_2$Cl] reacted with PPh_2Py in a non-polar solvent like benzene under refluxing conditions to afford *P*-coordinated neutral complex [(η^5-C_5H_5)Ru(κ^1-*P*-PPh_2Py)(PPh_3)Cl] (**1**). However, its reaction with PPh_2Py in a polar solvent methanol gave cationic complex containing both the PPh_3 and chelated PPh_2Py, [(η^5-C_5H_5)Ru(κ^2-*P*-*N*-PPh_2Py)(PPh_3)]$^+$ **1a.** Coordinated PPh_2Py in complex **1** exhibits monodentate behavior. In presence of NH_4PF_6 in methanol under stirring conditions at room temperature it gave chelated-*P*,*N* complex [(η^5-C_5H_5)Ru(κ^2-*P*-*N*-PPh_2Py)(PPh_3)]$^+$ (**1a**) in reasonably good yield. In CH_3CN, **1** afforded cationic complex [(η^5-C_5H_5)Ru(κ^1-*P*-PPh_2Py)(PPh_3)(CH_3CN)]BF_4 (**1b**) which was isolated as tetrafluoroborate salt.

Upon treatment with NaCN, NH_4SCN and NaN_3 in methanol, **1** afforded neutral complexes [(η^5-C_5H_5)Ru(κ^1-*P*-PPh_2Py)(PPh_3)CN] (**1c**), [(η^5-C_5H_5)Ru(κ^1-*P*-PPh_2Py)(PPh_3)NCS] (**1d**) and [(η^5-C_5H_5)Ru(κ^1-*P*-PPh_2Py)(PPh_3)(N_3)] (**1e**), respectively. Further, its reaction with *N*,*N*-donor chelating ligands viz., dimethylglyoxime (H_2dmg) and 1,2-phenylenediamine (pda) afforded cationic species [(η^5-C_5H_5)Ru(κ^1-*P*-PPh_2Py)(PPh_3)(κ^2-dmg)]$^+$ and [(η^5-C_5H_5)Ru(κ^1-*P*-PPh_2Py)(PPh_3)(κ^2-pda)]$^+$, which were isolated as tetrafluoroborate salt (**1e**) and (**1f**). A schematic representation showing the synthesis of complexes **1a–1g** is depicted in Scheme 1.

The complexes (**1–1g**) are air stable non-hygroscopic crystalline solids, soluble in polar solvents such as chloroform and dichloromethane, but insoluble in non-polar solvents benzene, hexane and *n*-pentane, diethyl ether and petroleum ether. All the complexes gave satisfactory elemental analyses. Formation of the complexes **1b**, **1c**, **1d** and **1e** were supported by the appearance υ($NCCH_3$), υ(CN^-), υ(N_3^-) and υ(SCN^-) asymmetric stretching vibrations as strong bands at 2324, 2227, 2043, and 2100 cm^{-1}, respectively [42,43]. Infrared spectra of the complex (**1f**) showed a sharp band at ~1030 cm^{-1} which is assigned to the υ(N–O) vibration and υ(O–H) stretches in this complex appeared at ~3400 cm^{-1} [44].

Information about composition of the complexes has also been obtained from FAB/ESI mass spectral studies. Resulting data along with their assignments are recorded in the experimental section and representative spectra of **1**, **1a**, **1e** and **1f** is depicted in Figs. S1–S4. Position of the various peaks and overall fragmentation patterns in the mass spectra of complexes conformed well to their respective formulations.

3.1. X-ray crystallography

Molecular structures of**1, 1a, 1c, 1e**, and **1f** has been determined crystallographically. Details about data collection, solution and refinement are recorded in Table 1, respectively. Molecular structures of **1, 1a, 1c, 1e**, and **1f** with atom numbering scheme is depicted in Figs. 1–5 and important geometrical parameters (bond lengths and bond angles) are summarized below the respective Figs. 1–5. A common structural feature of the complexes **1, 1a, 1c, 1e**, and **1f** is analogous arrangement of various groups about the metal center ruthenium. In all these complexes it adopted typical "piano stool" geometry. A peculiar structural feature of the PPh_2Py containing complexes **1** and **1a** is the coordination mode of PPh_2Py to the ruthenium center. In complex **1** it is bonded to the metal center ruthenium through phosphorus donor atom only, the nitrogen donor site [N1] is uncoordinated. The metal center ruthenium is coordinated to two P atoms one each from PPh_3

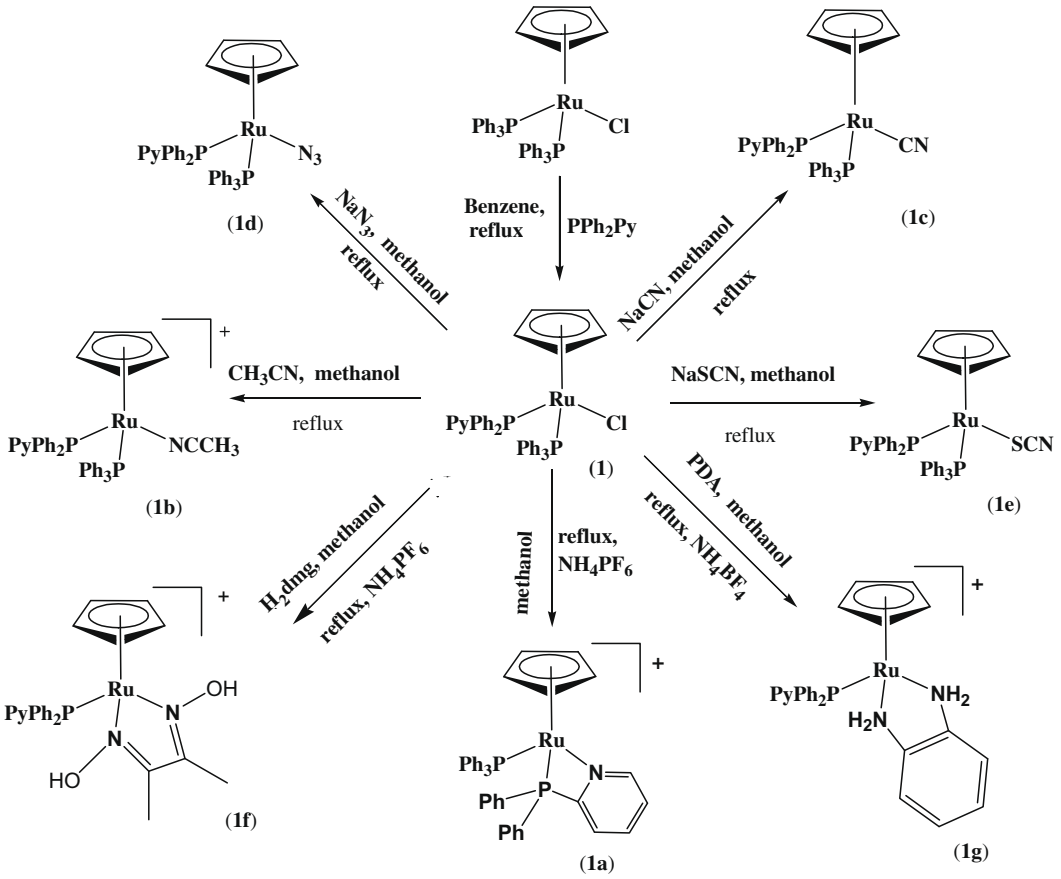

Scheme 1.

Table 1
Crystallographic data for the complexes **1**, **1a**, **1c**, **1e** and **1f**.

	1	1a	1c	1e	1f
Chemical formula	$C_{41}H_{35}Cl_4NP_2Ru$	$C_{40}H_{34}F_6N_2P_3Ru$	$C_{42}H_{36}Cl_2N_2P_2Ru$	$C_{41}H_{34}N_2P_2RuS$	$C_{27}H_{29}Cl_2F_6N_3O_2P_2Ru$
Formula weight	846.51	836.70	802.64	749.78	775.44
Color, habit	Orange, block	Brown, block	Orange, block	Brown, block	Orange, block
Crystal size (mm)	0.34 × 0.28 × 0.24	0.34 × 0.28 × 0.26	0.34 × 0.28 × 0.25	0.34 × 0.28 × 0.25	0.23 × 0.18 × 0.14
space group	$P\bar{1}$	Pn	$P\bar{1}$	$P21/c$	$P\bar{1}$
Crystal system	Triclinic	Monoclinic	Triclinic	Monoclinic	Triclinic
a (Å)	9.9190(2)	10.008(2)	9.7679(8)	13.3922(16)	11.026(2)
b (Å)	13.8668(4)	10.755(2)	13.9785(12)	18.671(2)	11.471(2)
c (Å)	14.4518(3)	17.422(4)	14.1604(12)	27.965(3)	13.583(3)
α (°)	99.588(2)	90.00	100.6340(10)	90.00	86.770(3)
β (°)	107.093(2)	94.59(3)	104.6820(10)	101.742(3)	68.355(3)
γ (°)	100.561(2)	90.00	98.5180(10)	90.00	87.283(3)
V (Å^3)	1815.66(7)	1869.3(7)	1799.2(3)	6846.2(14)	1593.7(5)
Z	2	4	2	4	2
D_{calc} (g cm^{-3})	1550	2.987	1.482	0.716	1.616
μ (mm^{-1})	0.847	1.217	0.707	0.322	0.825
T (K)	150(2)	293(2)	293(2)	293(2)	293(2)
Number of reflections	6371	7472	6212	16 796	5540
Number of parameters	446	461	442	848	398
R factor all	0.0274	0.0457	0.0464	0.1411	0.0648
R factor [$I > 2\sigma(I)$]	0.0222	0.0397	0.0409	0.0719	0.0593
WR_2	0.0570	0.1274	0.1289	0.2369	0.1701
WR_2 [$I > 2\sigma(I)$]	0.0554	0.1132	0.1111	0.1627	0.1630
Goodness-of-fit (GOF)	0.972	0.944	1.094	1.078	1.033

and PPh_2Py, the chloro group and cyclopentadienyl ring η^5-manner. Considering coordination of the cyclopentadienyl ring as occupying three-coordination sites in η^5-manner, overall geometry about ruthenium in the complex is typical "piano stool" geometry. It is further supported by bond angles between other ligands about the metal center [P(2)–Ru(1)–Cl(1) 90.260° and P(2)–Ru(1)–Cl(1)

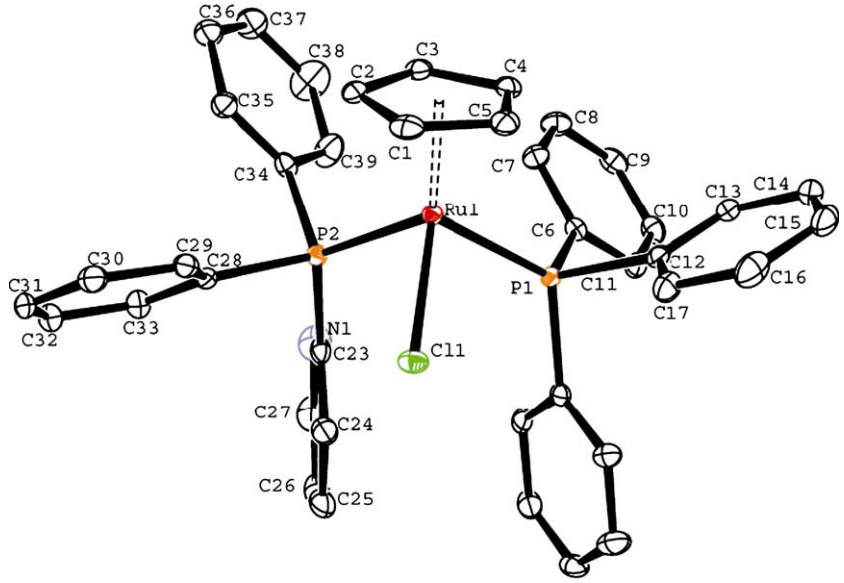

Fig. 1. Molecular structure of complex **1** and Selected bond length and angles (°): Ru(1)–P(1) 2.3187(5), Ru(1)–P(2) 2.3158(5), Ru(1)–Cl(1) 2.4523(5), Ru(1)–C(1) 2.223(2), Ru(1)–C(2) 2.2204(19), Ru(1)–C(3) 2.1785(19), Ru(1)–C(4), 2.1808(19), Ru(1)–C(5), 2.2237(19), P(1)–Ru(1)–Cl(1) 90.26(2), P(2)–Ru(1)–Cl(1) 90.72(2), P(2)–Ru(1)–P(1) 100.76(2).

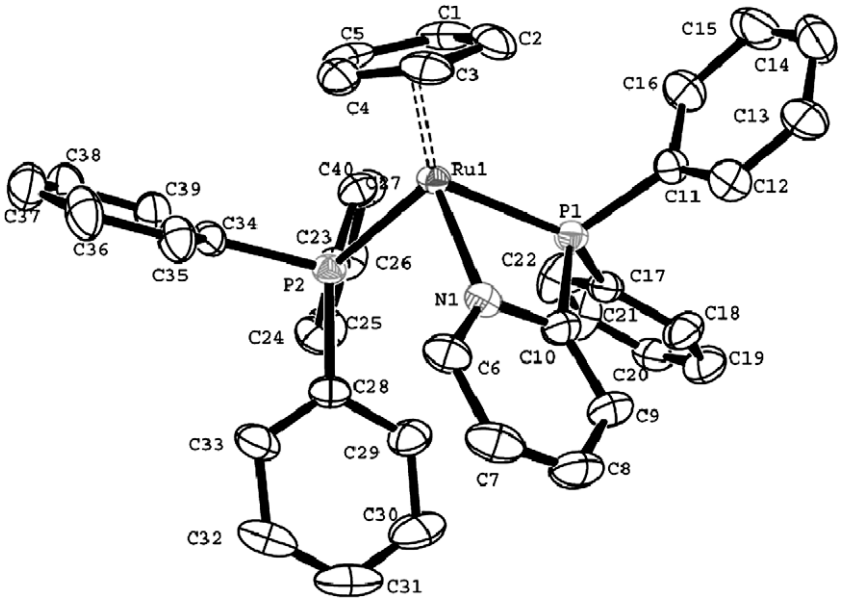

Fig. 2. Molecular structure of complex **1a** and Selected bond length (Å) and angles (°): Ru(1)–N(1) 2.148(4), Ru(1)–P(1) 2.3024(13, Ru(1)–P(2) 2.3021(13), Ru(1)–C(1) 2.182(6), Ru(1)–C(2) 2.220(6), Ru(1)–C(3) 2.233(5), Ru(1)–C(4), 2.215(6), Ru(1)–C(5), 2.187(6), N(1)–Ru(1)–P(1) 67.20(1), N(1)–Ru(1)–P(2) 90.24(12), P(1)–Ru(1)–P(2) 102.72(5).

90.718°)]. The Ru(1)–Cl(1) bond distance in **1** is 2.4523(5) Å, close to the values reported in literature [45–48]. The Ru(1)–P(1), and Ru(1)–P(2), bond distances are 2.3187(5), and 2.3158(5) Å and are normal [45–49]. The η^5-C_5H_5 ring is planar and average bond distance between ruthenium and centroid of the η^5-C_5H_5 ring is 1.845 Å.

Overall coordination geometry about the ruthenium center in **1a** is analogous to that in **1** except that Cl has been replaced by uncoordinated pyridyl nitrogen of PPh_2Py. In **1a**, PPh_2Py is coordinated to ruthenium as a chelating *P,N*-donor ligand forming a four membered chelate ring with a bite angle of 67.20(2)°. The Ru–P bond distances 2.3024(13) Å are slightly shorter than in **1**. The Ru(1)–N(1) bond distance of 2.148(4) Å in this complex falls within the range reported for Ru–N bond distances [50,51]. The bond distance between nitrogen and phosphorus atoms of PPh_2Py is approximately 2.40 Å and the distance between ruthenium and centroid of the η^5-C_5H_5 ring is 1.854 Å, which is similar to that in **1**.

Complexes **1c** and **1e** which were obtained by displacement of Cl^- in **1** by CN^- and SCN^-, respectively displayed analogous structural features as observed in the precursor complex. The Ru(1)–$C(41)_{CN}$ and Ru(1)–$N(1)_{SCN}$ bond distances in complexes **1c** and **1e** are 2.000(4) and 2.083(6) Å, respectively, while Ru–P bond distances of 2.3407(13) Å falls within the range of Ru–P distances reported in the literature [45–52]. The average bond distance between ruthenium and centroid of the ring is exactly the same as in **1**. The bond angles C(41)–Ru(1)–P(1), and C(41)–Ru(1)–P(2)

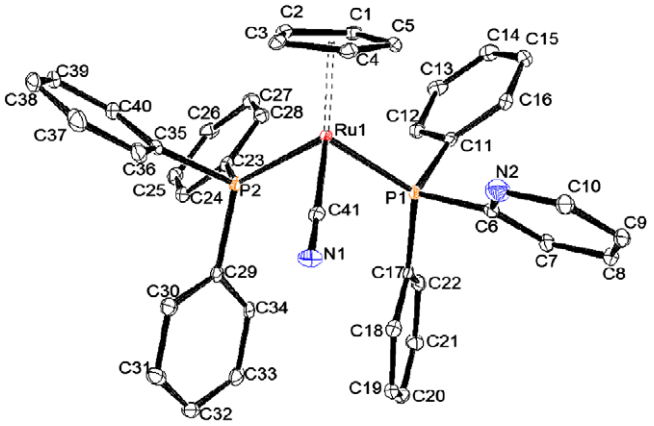

Fig. 3. Molecular structure of complex **1c** and Selected bond length (Å) and angles (°): Ru(1)–P(1) 2.2916(9), Ru(1)–P(2) 2.3112(9), Ru(1)–C(41) 2.000(4), Ru(1)–C(1) 2.241(3), Ru(1)–C(2) 2.230(3), Ru(1)–C(3) 2.246(3), Ru(1)–C(4), 2.241(3), Ru(1)–C(5), 2.229(3), C(41)–N(1)–Ru(1) 174.4(3), P(2)–Ru(1)–P(1) 102.94(3), C(41)–Ru(1)–P(1) 89.35(10), C(41)–Ru(1)–P(2) 87.20(10).

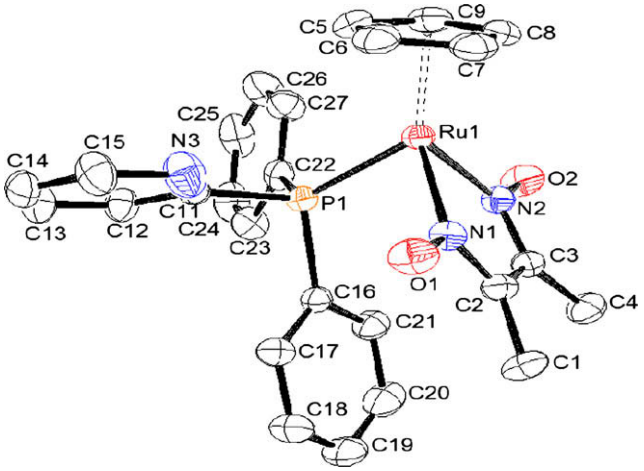

Fig. 5. Molecular structure of complex **1f** and Selected bond length (Å) and angles (°): Ru(1)–N(1) 2.046(4), Ru(1)–N(2) 2.034(4), Ru(1)–P(1) 2.3407(13), Ru(1)–C(5) 2.193(5), Ru(1)–C(6) 2.209(5), Ru(1)–C(7) 2.200(6), Ru(1)–C(8), 2.200(5), Ru(1)–C(9), 2.198(5), N(2)–Ru(1)–N(1), 73.40(16), C(2)–N(1)–Ru(1) 120.4(3), C(3)–N(2)–Ru(1) 121.0(3), N(1)–Ru(1)–P(1) 90.10(12), N(2)–Ru(1)–P(1) 89.95(13), O(1)–N(1)–Ru(1) 125.4(3), O(2)–N(2)–Ru(1) 125.3(3).

in **1c** are 89.35(10) and 87.20(10)°, while the bond angles N(1)–Ru(1)–P(1) and N(2)–Ru(1)–P(2) in **1e** are 89.78(16) and 94.78(16)°, respectively, suggesting a "piano stool" structure.

In complex **1f** the metal center ruthenium is bonded to PPh_2Py through phosphorus atom in monodentate fashion, dimethylglyoxime (H_2dmg) through both the nitrogen donor atoms and cyclopentadienyl ring in η^5-manner. In this complex also, overall geometry about the ruthenium center is typical "piano stool" geometry. Dimethylglyoxime ligand is coordinated to ruthenium as a bidentate *N*,*N*-donor ligand forming five-membered chelate ring with a bite angle of 73.39(2)°. In **1f** the Ru–P bond distance is 2.3407(13) Å, and Ru(1)–N(1) and Ru(1)–N(2) bond distances are 2.046(4) and 2.034(4) Å, respectively, shorter than Ru(II)–N lengths where N-donor ligand is not involved in π-interaction with the metal center [53–56]. The C–N lengths within the coordinated dioxime ligands are also significantly longer than localized C=N bond [57]. The decrease in Ru–N distance and increase in C–N distance within the ruthenium–dioxime chelate clearly indicate strong π-interaction between ruthenium and the diimine fragment of the dioxime ligands. The bond angles around the ruthenium are N(1)–Ru–P(1) 90.10(12), N(2)–Ru–P(1) 89.95(13), and N(2)–Ru(1)–N(1) 73.40(5)°.

Crystal structure of complexes**1, 1a, 1c, 1e**, and **1f** displayed the presence of extensive intra- and intermolecular C–H···X (X = N, Cl, and F) and C–H···π interactions. These types of interactions play significant role in the building of huge supramolecular moieties [58]. Some interesting motifs resulting from weak bonding interactions in **1a** and **1f** are shown in Figs. 6 and 7, respectively.

3.2. ^1H and ^{31}P NMR spectral studies

Coordination of PPh_2Py to metal center ruthenium is evident from shifts in the position of resonances associated with various

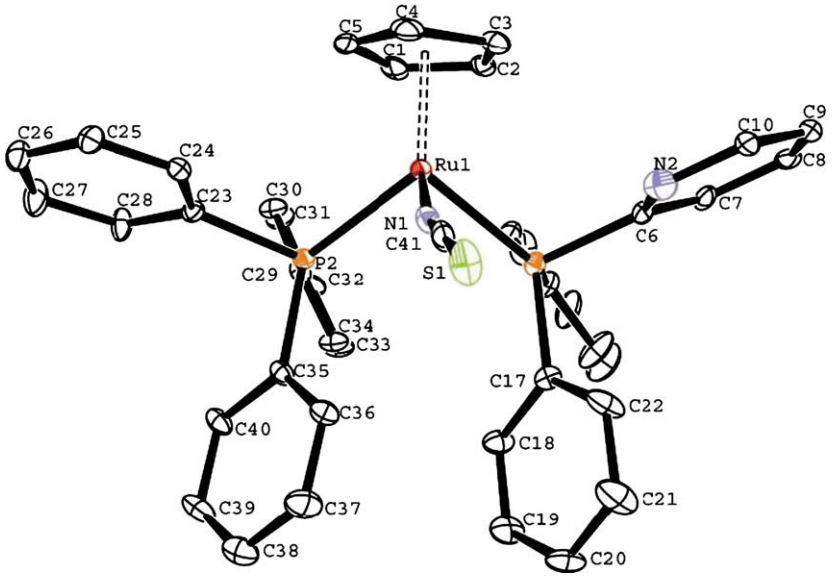

Fig. 4. Molecular structure of complex **1e** and Selected bond length (Å) and angles (°): Ru(1)–N(1) 2.083(6), Ru(1)–P(1) 2.3031(18), Ru(1)–P(2) 2.3174(17), Ru(1)–C(1) 2.197(7), Ru(1)–C(2) 2.177(6), Ru(1)–C(3) 2.189(6), Ru(1)–C(4), 2.214(7), Ru(1)–C(5), 2.223(8), C(41)–N(1)–Ru(1) 168.4(6), N(1)–Ru(1)–P(1) 89.78(16), N(1)–Ru(1)–P(2) 94.31(16), P(1)–Ru(1)–P(2) 94.31(16).

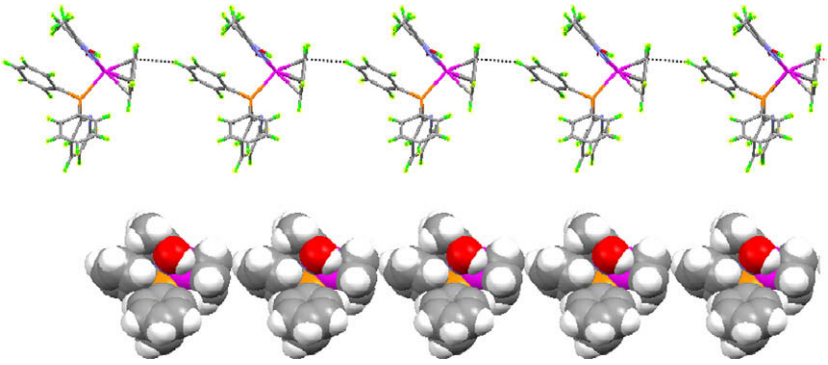

Fig. 6. Straight chain motif resulting from C–H···π interactions [2.839 Å] in **1f**.

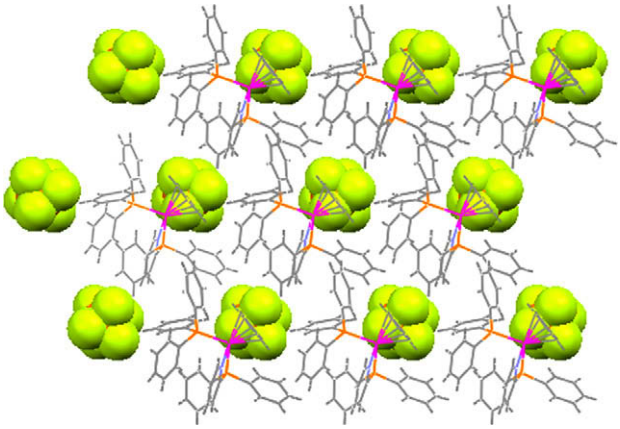

Fig. 7. Counter anion (PF_6^-) encapsulated in self-assembled cavity of complex **1a**.

protons and signal corresponding to ^{31}P nuclei compared to that in the precursor complex $[(\eta^5\text{-}C_5H_5)Ru(PPh_3)_2Cl]$. ^1H NMR spectrum of **1** displayed a singlet at δ 4.70 ppm corresponding to chemically equivalent protons of $\eta^5\text{-}C_5H_5$, which exhibited a downfield shift compared to that in the starting compound. This downfield shift may be attributed to the substitution of one PPh_3 by PPh_2Py. The resonances in the aromatic region at δ 7.32–7.82 ppm have been assigned to the aromatic and pyridyl protons of phosphine ligands. The ^{31}P NMR displayed one singlet at δ 25.88 ppm corresponding to the ^{31}P nuclei of phosphine ligand. The signal associated with ^{31}P nuclei exhibited a significant downfield shift upon coordination to the metal as compared to that in the free ligand (−3.43 ppm). The ^1H NMR spectrum of **1a** exhibited a quite different pattern of signals from the one observed in the spectrum of **1**. In this complex the pyridine ring protons appeared as triplets at δ 7.89 and 8.01 and a doublet at δ 8.67 ppm. The phenyl group protons resonated as a broad multiplet in the aromatic region at δ 7.09–7.79 ppm. The $\eta^5\text{-}C_5H_5$ protons resonated as a singlet at δ 5.08 ppm. It exhibited a downfield shift compared to that in complex **1** In it's $^{31}P\{^1H\}$ NMR spectrum complex **1a** exhibited a singlet in the high field side at −11.36 ppm and a singlet at 41.54 ppm. The singlet in the high field side has been attributed to the ^{31}P nuclei of PPh_2Py while the one at 41.54 ppm to the PPh_3. The upfield shift in position of the signal associated with ^{31}P nuclei may be due enhanced back-bonding to the PPh_2Py on going from monodentate to chelating coordination mode.

^1H NMR spectrum of **1b** exhibited a singlet associated with methyl protons of acetonitrile at δ 2.18 ppm along with the signals due to $\eta^5\text{-}C_5H_5$ and phosphine protons. The ^{31}P nuclei in this complex resonated at δ 40.04 ppm. ^1H NMR spectrum of the complex **1g** exhibited two doublets at δ 7.16 and 8.23 ppm corresponding to ring protons of 1,2-phenylenediamine and showed broad peak around δ 4.5–5.0 ppm due to coordinated NH_2 group along with the signals associated with $\eta^5\text{-}C_5H_5$ and aromatic protons of phosphine. An isolated signal observed near 10.5 ppm in the complex (**1f**) has been assigned to the oxime –OH proton. The methyl protons of the coordinated dimethylglyoxime in $[(\eta^5\text{-}C_5H_5)Ru(\kappa^1\text{-}P\text{-}PPh_2Py)(H_2dmg)]^+$ (**1f**) were displayed as a sharp singlet at δ 1.92 ppm.

3.3. Electronic spectral studies

The complexes under study exhibited absorptions in visible and ultraviolet region. UV–Vis absorption spectral data of **1–1g** is recorded in the experimental section and representative spectra of [1]BF_4, **–[1g]**BF_4 is depicted in Fig. 8. The electronic spectra of **1a–1g** in dichloromethane displays UV–Vis pattern similar to the analogous ruthenium polypyridyl complexes [58]. Ruthenium cyclopentadienyl complexes usually show intense peaks in the UV region corresponding to ligand-based π–π* transitions with the overlapping metal-to-ligand (MLCT) transitions in the visible region. An analogous general trend is observable in the electronic spectra of the complexes under study. Complexes **1–1g** displayed intense transitions in the UV–Vis region. The lowest energy absorption bands in the electronic spectra of **1–1g** in visible region at ∼478–557 and 403–373 nm on the basis of its intensity and the position have tentatively assigned to $M_{d\pi\rightarrow L^*}$ metal-to-ligand charge transfer transitions (MLCT). The bands in the high-energy side at ∼ 250–260 nm have been assigned to the intra-ligand $\pi\rightarrow\pi^*/n\rightarrow\pi^*$ transitions [59,60]. Significantly destabilizes the π^* orbital of the cyclopentadienyl, resulting in the blue-shifted $M_{d\pi\rightarrow L^*}$ absorption bands. However, substitution of the chloro group by anionic ligands like SCN^-, N_3^- has little influence on the MLCT bands.

3.4. Electrochemistry

Electrochemical behavior of the complexes are very similar to the polypyridyl complexes of ruthenium(II) and has been rationalized in terms of a metal and ligand-based reactions. Electrochemical properties of **1a**, and **1f** were followed by cyclic voltammetry. The study was performed in acetonitrile solution (0.1 M TBAP) at room temperature (scan rate 100 mV/s). Representative voltammogram of complex **1a** is shown in Fig. 9. Complex **1a** exhibits an oxidative response on the positive side of glassy carbon electrode in the range 0.20–0.55 V, while **1f** shows in the range of 0.30–0.80 V, which has been assigned to Ru(II)/Ru(III) oxidation (Fig. S5). This oxidation in **1a** is reversible and characterized by a peak-to-peak separation (δEp) of ∼100 mV and the anodic peak

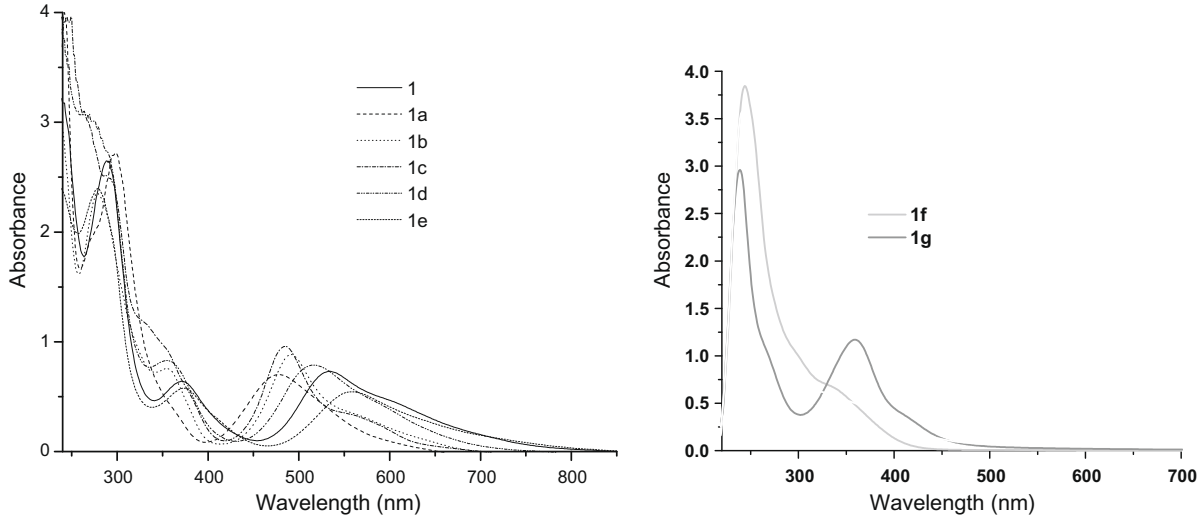

Fig. 8. (a) UV–Vis spectra of complexes **1–1e** (b) UV–Vis spectra of complexes **1f** and **1g**.

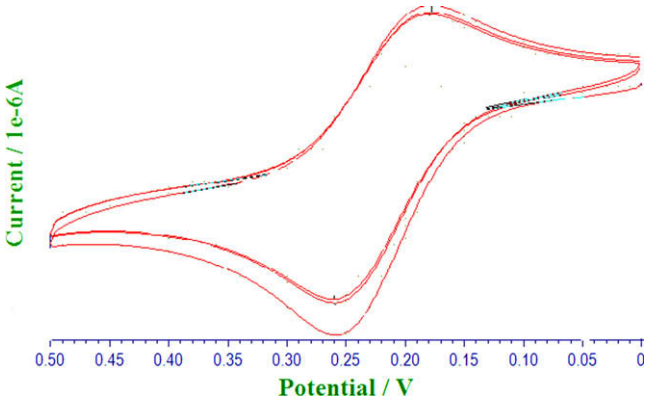

Fig. 9. Cyclic voltammogram of complex **1a**.

current (i_{pa}) is almost equal to cathodic peak current (i_{pc}) which is expected for a reversible electron-transfer process. The reversible reduction peak at −0.53 V has been attributed to the Ru(II)/Ru(I) redox process. Complex **1f** exhibited irreversible oxidation peak at 0.76 V and two reversible reduction peaks at −0.4 and −1.4 V which can be assigned to the stepwise reduction of the dimethylglyoxime. Similar behavior, i.e. reversible III/II (**1a**) and irreversible II/I (**1f**) processes, has been observed in $RuCl_2(CO)(PR_3)_3$ and $RuCl_2(CO)_2(PR_3)_2$ systems [30]. As expected additional π-acceptors present in the carbonyl species leads to higher reduction potentials compared to the values found in **la** and **1f**. The one-electron nature of this oxidation was established by comparing its current height with that of the standard ferrocene/ferrocenium couple under identical experimental conditions. The ruthenium(II)–ruthenium(III) oxidation potential in these $[(\eta^5\text{-}C_5H_5)\text{-}Ru(\kappa^2\text{-}P,N\text{-}PPh_2Py)(PPh_3)]^+$ (**1a)** is lower than that in $[(\eta^5\text{-}C_5H_5)\text{-}Ru(PPh_3)_2Cl]$ (0.70 V), which shows that there will be high electron density on the metal center, one can expect that the degree of back-bonding increases metal-to-ligand pπ–dπ interaction.

3.5. Catalytic transfer hydrogenation of aldehydes

To evaluate selectivity and efficacy of the complex **1** towards reduction of mono/di formyl group aldehyde was used as model substrate. Hydrogenation was initiated by introducing formic acid, sodium acetate and aldehydes (1.0 mmol) in water (a few drops of freshly distilled acetonitrile was used to dissolve the catalyst) and air at 80 °C with 2 mol% of the catalyst. The data indicated that complex **1** is reasonably efficient hydrogen-transfer catalyst under aerobic conditions. It catalyzes hydrogenation of different aldehydes or substituted aldehydes (Benzaldehyde, 4-Methylbenzaldehyde, 4-Nitrobenzaldeyde, 4-Cyanobenzaldehyde, Terephthaldialdehyde), to produce alcohols or substituted alcohols in aqueous solution (Table 2). It is believed that active species in the present case is probably a 16 electron species derived from complex **1** by loss of a phosphine ligand [61]. It was observed that in all these cases formyl group of aldehydes were selectively reduced without affecting other groups (CN, NO_2), while in cases of terephthaldialdehyde only one formyl group was selectively reduced. From the table it is clear that catalytic conversion of the aldehydes to corresponding alcohols are based on electron withdrawing and electron donating substituents i.e., $NO_2^- > CN^- > CH_3^-$ on the basis of nucleophilic addition reaction shown in Scheme 2. Further, it was observed that complex **1** leads to almost 90% conversion of aldehyde into corresponding alcohol in 6–8 h, expect 4-methylbenzaldehyde wherein reactivity towards reduction process is poor. It may be attributed to the presence of electron donating methyl group, which decreases the electrophilicity of the carbonyl carbon in corresponding aldehyde. The corresponding alcohols have been characterized by both IR and ^1H NMR spectroscopy, and percentage conversions were calculated on the basis of integration of peaks in the NMR.

In the course of our study on planar–chiral complexes of late transition metal, we prepared planar–chiral Cp-phosphine ruthenium complex $[Ru(Cp)(PPh_2Py)PPh_3Cl]$ **1**, in which anchor phosphine prevents the rotation of the Cp ring, constructing a good asymmetric environment around the ruthenium metal. Efficiency of the planar–chiral Cp-phosphine ligand was proved by the induction of metal-centered chirality with a high selectivity in the ligand exchange reactions with phosphine (PPh_2Py) and anionic/neutral ligands. Since the complexes **1–1e** possess chiral center around metal ion. Since priority order of the ligands for the Ru center falls in the order Cp > L > P_1 > P_2/, therefore the complexes **1**–**1e** exhibits *R* configuration around the Ru centers. (L = $NCCH_3$, N_3, SCN, P_1 = PPh_2Py, P_2 = PPh_3). Selectivity of the conversion of aldehydes using complex **1** as catalyst is quite high, producing corresponding alcohols exclusively. It is reasonable to consider that the first step of the net reaction is hydrogenation of aldehydes (addition of nucleophile H^-) to form corresponding alcohols, following the nucleophilic addition mechanism.

Table 2
Transfer-Hydrogenation of Substrate catalyzed by complex 1 in acetonitrile at 85 °C, 2 mol% catalyst and reaction time of 6–12 h.

Substrate	Structure	Products	Time(h)	Yield[a] (%)	TOF[b] (h^{-1})
Benzaldehyde	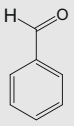	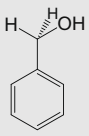	6	90	9.1
4-Methylbenzaldeyde	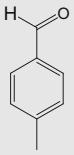	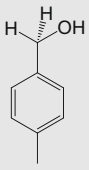	12	35	1.4
4-Nitrobenzaldeyde	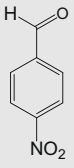	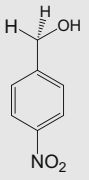	3	95	15.8
4-Cyanobenzaldeyde	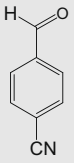	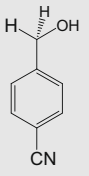	3	92	15.3
Terephthaldialdehyde	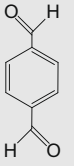	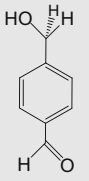	8	92	5.75

[a] Isolated yields after column chromatography.
[b] Based on percentage of yields.

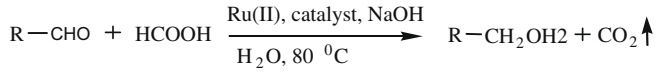

(R=benzaldehyde, 4-methylbenzaldehyde, 4-nitrobenzaldeyde, 4-cyanobenzaldehyde, terephthaldialdehyde).

Scheme 2.

4. Conclusion

Through this work we have reported new chiral η^5-cyclopentadienyl ruthenium(II) complexes containing diphenyl-2-pyridylphosphine alongwith monodentate ligand. The coordinated PPh_2Py exhibits mono/chelating behavior. Furthermore, it has been shown that the complex **1** effectively catalyze reduction of aldehydes or substituted aldehydes into corresponding alcohol and it serves as an effective hydrogenating catalyst for the use in water and air and delivers faster rates in absence of inert gas protection or substrate solubility in water.

Acknowledgements

We gratefully acknowledge financial support from the Department of Science and Technology, Ministry of Science and Technology, New Delhi, India (Grant No. SR/SI/IC-15/2007). Thanks are also due to Prof. P. Mathur, In-charge, National Single Crystal X-ray diffraction Facility, Indian Institute of Technology, Mumbai, and Prof. P.K. Bhardwaj, In-charge, National Single Crystal X-ray diffraction Facility, Indian Institute of Technology Kanpur for providing single X-ray data. Further, we are grateful to the Head, Department of Chemistry, Faculty of Science, Banaras Hindu University, Varanasi, for extending laboratory facilities.

Appendix A. Supplementary material

CCDC 718816, 718817, 718818, 718819 and 718820 contains the supplementary crystallographic data for complexes **1**, **1a**, **1c**, **1e** and **1f**. These data can be obtained free of charge from The Cambridge Crystallographic Data Centre via http://www.ccdc.cam.ac.uk/data_request/cif.

Supplementary data associated with this article can be found, in the online version, at doi:10.1016/j.jorganchem.2009.07.011.

References

[1] Z. Xie, Acc. Chem. Res. 36 (2003) 1.
[2] H.L. Bozec, D. Touchard, P.H. Dixneuf, Adv. Organomet. Chem. 29 (1989) 163.
[3] P.M. Maitlis, J. Organomet. Chem. 500 (1995) 239.
[4] E.W. Abel, F.G.A. Stone, G. Wilkinson (Eds.), Comprehensive Organometallic Chemistry II: A Review of the Literature, 1982–1994, p. 8177.
[5] J. Halpern, B.M. Trost, Proc. Natl. Acad. Sci. USA 101 (2004) 5347.
[6] I. Ojima (Ed.), Catalytic Asymmetric Synthesis, second ed., Wiley, VCH, New York, 2000.
[7] E.N. Jacobsen, A.P. Faltz, H. Yamamoto (Eds.), Comprehensive Asymmetric Catalysis, Springer, Berlin, 1999.
[8] R. Noyori, Asymmetric Catalysis in Organic Synthesis, John Wiley and Sons, New York, 1994.
[9] K. Drauz, H. Waldmann (Eds.), Enzyme Catalysis in Organic Synthesis: A Comprehensive Handbook, second ed., vol. I–III, Wiley-VCH, Weinheim, 2002.
[10] K. Faber, Biotransformations in Organic Chemistry, fourth ed., Springer, Berlin, 2000.
[11] P.I. Dalko, L. Moisan, Angew. Chem. Int. Ed. 43 (2004) 138.
[12] C.S. Hauser, C. Slugove, K. Mereiter, R. Schimid, K. Kirchner, L. Xiao, W. Weissenteiner, J. Chem. Soc., Dalton Trans. (2001) 2989.
[13] A. Furstner, M. Picquet, C. Bruneau, P.H. Dixneuf, Chem. Commun. (1998) 315.
[14] B.C.G. Soderberg, Coord. Chem. Rev. 241 (2003) 147.
[15] C.S. Allardyce, P.J. Dyson, D.J. Ellis, S.L. Heath, Chem. Commun. (2001) 1396.
[16] H. Chen, J.A. Parkinson, S. Parsons, R.A. Coxall, R.O. Gould, P.J. Sadler, J. Am. Chem. Soc. 124 (2003) 3064.
[17] R.E. Aird, J. Cummings, A.A. Ritchie, M. Muir, R.E. Morris, H. Chen, P.J. Sadler, D.I. Jodrell, Br. J. Cancer 86 (2002) 1652.
[18] R.E. Morris, R.E. Aird, P.D.S. Murdoch, H. Chen, J. Cummings, N.D. Hughes, S. Parsons, A. Parkin, G. Boyd, D.I. Jodrell, P.J. Sadler, J. Med. Chem. 44 (2001) 3616.
[19] F. Bottomley, Coord. Chem. Rev. 7 (1978) 26.
[20] P. Jutzi, T. Redeker, Eur. J. Inorg. Chem. (1998) 663.
[21] P. Jutzi, U. Siemeling, J. Organomet. Chem. 500 (1995) 175.
[22] U. Siemeling, Chem. Rev. 100 (2000) 1495.
[23] H. Butenschon, Chem. Rev. 100 (2000) 1527.
[24] M.E. Zhao, J.Li. Mano, Z. Song, D.M. Tschaen, E.J.J. Grabowski, P.J. Reider, J. Org. Chem. 64 (1999) 2564.
[25] N.W. Alcock, P. Moore, P.A. Lampe, K.F. Mock, J. Chem. Soc., Dalton Trans. 207 (1982).
[26] M.M. Olmstead, A.J.P. Maisonnat Farr, A.L. Balch, Inorg. Chem. 20 (1981) 4060.
[27] Y. Inoguchi, B. Milewski-Marla, H. Schmidbauer, Chem. Ber. 115 (1982) 3085.
[28] J.P. Parr, M.M. Olamstead, F.E. Wood, A.L. Balch, J. Am. Chem. Soc. 97 (1983) 77.
[29] H.J. Wasserman, D.C. Moody, R.T. Paine, R.R. Ryan, K.V. Salazar, J. Chem. Soc., Chem. Commun. 533 (1984).
[30] E.B. Milosavljevic, Lj. Solujic, D.W. Krassowski, J.H. Nelson, J. Organomet. Chem. 352 (1988) 177.
[31] F.E. Hong, Y.C. Chang, R.E. Chang, C.C. Lin, S.L. Wang, F.L. Liao, J. Organomet. Chem. 588 (1999) 160.
[32] F.E. Wood, M.M. Olamstead, J.P. Farr, A.L. Balch, Inorg. Chim. Acta 97 (1985) 77.
[33] U. Abram, R. Alberto, J.R. Dilworth, Y. Zheng, K. Ortner, Polyhedron 18 (1999) 2995.
[34] D. Drommi, C. Arena, Nicolo, F.G. Bruno, F. Faraone, J. Organomet. Chem. 485 (1995) 115.
[35] J. Goubean, W.Á. Bues, Zngor. Ally. Chem. 268 (1952) 221.
[36] B.M. Trost, Chem. Ber. 129 (1996) 1313–1322;
B.M. Trost, F.D. Toste, A.B. Pinkerton, Chem. Rev. 101 (2001) 2067–2096.
[37] B.M. Trost, M.U. Frederiksen, M.T. Rudd, Angew. Chem. 117 (2005) 6788–6825;
B.M. Trost, M.U. Frederiksen, M.T. Rudd, Angew. Chem. Int. Ed. 44 (2005) 6630–6666.
[38] D.D. Perrin, W.L.F. Armango, D.R. Perrin, Purification of Laboratory Chemicals, Pergamon, Oxford, UK, 1986.
[39] M.I. Bruce, C. Hameister, A.G. Swincer, R.C. Wallis, Inorg. Synth. 21 (1982) 78.
[40] G.M. Sheldrick, SHELX-97: Programme for the solution and refinement of crystal structures, University of Göttingen, Germany, 1997.
[41] A.L. Spek, Acta Crystallogr. 46 (1990) C31.
[42] W.D. Stalleup, D. Williams, J. Chem. Phys. 10 (1942) 199.
[43] D. Seybold, K.Z. Dehnicke, Anorg. Allg. Chem. 361 (1968) 277.
[44] L.H. Jones, J. Chem. Phys. 22 (1954) 217.
[45] M. Chandra, A.N. Sahay, D.S. Pandey, R.P. Tripathi, J.K. Saxena, V.J.M. Reddy, M.C. Puerta, P. Valerga, J. Organomet. Chem. 689 (2004) 2256.
[46] W.J. Perez, C.H. Lake, R.F. See, L.M. Toomey, M.R. Churchill, K.J. Takeuchi, C.P. Radano, W.J. Boyko, C.A. Bessel, J. Chem. Soc., Dalton Trans. (1999) 2281.
[47] M.R. Churchill, K.M. Keil, F.V. Bright, S. Pandey, G.A. Baker, J.B. Keister, Inorg. Chem. 39 (2000) 5807.
[48] P. Ghosh, A. Chakravorty, Inorg. Chem. 36 (1997) 64.
[49] P. Paul, B. Tyagi, A.K. Bilakhia, P. Dastidar, E. Suresh, Inorg. Chem. 39 (2000) 14.
[50] T. Hayashida, H. Nagashima, Organometallics 21 (2002) 3884.
[51] H. Aneetha, P.S. Zacharias, B. Srinivas, G.H. Lee, Y. Wang, Polyhedron 18 (1999) 299.
[52] I. Moldes, E.D.L. Encarnacion, J. Ros, A.A. Larena, J.F. Piniella, J. Organomet. Chem. 566 (1998) 165.
[53] K.N. Mitra, P. Majumder, S.M. Peng, A. Castineiras, S. Goswami, Chem. Commun. (1997) 1267.
[54] R.C. Elder, M. Trkula, Inorg. Chem. 16 (1977) 1048.
[55] F.C. March, G. Ferguson, Can. J. Chem. 49 (1971) 3590.
[56] R.J. Sundberg, R.F. Bryan, I.F. Taylor, H. Taube, J. Am. Chem. Soc. 96 (1974) 381.
[57] D. Chattopadhya, S.K. Majumdar, T. Banerjee, S. Ghosh, Acta. Crystallogr., Sect. C. 44 (1988) 1025.
[58] C.D. Nunes, M. Pillinger, A. Hazell, J. Jepsen, T.M. Santos, J. Madureira, A.D. Lopes, I.S. Goncalves, Polyhedron 22 (2003) 2799.
[59] P. Kopel, Z. Travnicek, L. Kvitek, R. Panchartkova, M. Biler, M. Marek, M. Nadvornik, Polyhedron 18 (1999) 1779.
[60] S. Kar, T.A. Millar, S. Chakraborty, B. Sarkar, B. Pradhan, R.K. Singh, T. Kunda, M.D. Ward, G.K. Lahiri, Dalton Trans. (2003) 2591.
[61] R.A. Sbnchez-Delgado, N. Valencia, Rosa-Linda Mgrquez-Silva, A. Andriollo, M. Medina, Inorg. Chem. 25 (1986) 8.